Catal Lett (2012) 142:860–868
DOI 10.1007/s10562-012-0842-0

Methanation of Carbon Dioxide Over Mesoporous Nickel–M–Alumina (M = Fe, Zr, Ni, Y, and Mg) Xerogel Catalysts: Effect of Second Metal

Sunhwan Hwang · Ung Gi Hong · Joongwon Lee · Joon Hyun Baik · Dong Jun Koh · Hyojun Lim · In Kyu Song

Received: 7 April 2012 / Accepted: 7 May 2012 / Published online: 18 May 2012

Abstract Mesoporous nickel (35 wt%)–M (5 wt%)–alumina xerogel (denoted as 35Ni5MAX) catalysts with different second metal (M = Fe, Zr, Ni, Y, and Mg) were prepared by a single-step sol–gel method for use in the methane production from carbon dioxide and hydrogen. In the carbon dioxide methanation reaction, yield for CH_4 decreased in the order of 35Ni5FeAX > 35Ni5ZrAX > 35Ni5NiAX > 35Ni5YAX > 35Ni5MgAX. This indicated that the catalytic performance was greatly influenced by the identity of second metal in the carbon dioxide methanation reaction. Experimental results revealed that CO dissociation energy and metal-support interaction of the catalyst played key roles in determining the catalytic performance of 35Ni5MAX catalysts in the reaction. Among the catalysts tested, 35Ni5FeAX catalyst, which retained the most optimal CO dissociation energy and the weakest metal-support interaction, exhibited the best catalytic performance in terms of conversion of CO_2 and yield for CH_4.

Keywords Carbon dioxide methanation · Carbon dioxide · Hydrogen · Nickel–metal–alumina xerogel catalyst · Single-step sol–gel method

S. Hwang · U. G. Hong · J. Lee · I. K. Song (✉)
School of Chemical and Biological Engineering, Institute of Chemical Processes, Seoul National University, Shinlim-dong, Kwanak-ku, Seoul 151-744, South Korea
e-mail: inksong@snu.ac.kr

J. H. Baik · D. J. Koh
Environment Research Department, Research Institute of Industrial Science & Technology, Pohang 790-330, South Korea

H. Lim
POSCO, Gangnam-gu, Seoul 135-389, South Korea

1 Introduction

Synthetic natural gas (SNG) has attracted much attention with increasing demands for natural gas which is considered as a green and eco-friendly energy [1–3]. Among various chemical processes for the production of SNG, coal-to-SNG is known to be a promising process for producing SNG [4–6]. However, the coal-to-SNG process inevitably releases carbon dioxide into the atmosphere. Because carbon dioxide is known to be one of the greenhouse gases, various strategies such as separation, storage, and utilization of carbon dioxide are necessary to reduce the concentration of carbon dioxide in the coal-to-SNG process [7–9]. Among various strategies, methanation of carbon dioxide, which produces methane from carbon dioxide and hydrogen, not only reduces carbon dioxide but also increases yield for SNG. Carbon dioxide methanation reaction is interesting from ecological and economical viewpoints. Therefore, developing an efficient catalyst for carbon dioxide methanation reaction would be of great interest.

Methanation of carbon dioxide has been investigated over a number of catalysts based on VIIIB metals (for example, Ru, Rh, Ni, Co, and Fe) supported on various metal oxides (for example, SiO_2, Al_2O_3, ZrO_2, TiO_2, and CeO_2) [10, 11]. Among these catalysts, Ni-based catalysts have been widely employed for carbon dioxide methanation reaction due to their high catalytic activity and high selectivity for methane. However, it is known that conventional nickel-based catalysts suffer from severe catalyst deactivation in the carbon dioxide methanation reaction, because nickel particles are sintered during the exothermic methanation reaction [12]. To overcome this problem, addition of second metal such as Fe, Sm, Ce, La, Mg, and Y has been attempted to enhance the stability and catalytic

activity of nickel-based catalysts in the carbon dioxide methanation reaction [13–18].

It has been reported that a mesoporous nickel–alumina xerogel catalyst prepared by a single-step sol–gel method can serve as an efficient catalyst in several reactions due to well-developed mesoporosity and finely dispersed nickel species [19, 20]. However, any investigations on the carbon dioxide methanation reaction over mesoporous nickel–M–alumina xerogel catalysts with different second metal (M) have not been attempted yet. Therefore, a systematic investigation of mesoporous nickel–M–alumina xerogel catalysts for methanation reaction would be worthwhile.

In this work, a series of mesoporous nickel–M–alumina xerogel catalysts with different second metal (M = Fe, Zr, Ni, Y, and Mg) were prepared by a single-step sol–gel method, and they were applied to the methane production from carbon dioxide and hydrogen. The effect of second metal of mesoporous nickel–M–alumina xerogel catalysts on the physicochemical properties and catalytic performance in the methanation reaction was investigated. The nickel–M–alumina xerogel catalysts were characterized by BET, XRD, TPR, CO_2-TPD, H_2-TPD, TPSR, and TEM analyses.

2 Experimental

2.1 Preparation of Mesoporous Nickel–M–Alumina Catalysts

A series of mesoporous nickel–M–alumina xerogel catalysts with different second metal (M = Fe, Zr, Ni, Y, and Mg) were prepared by a single-step sol–gel method according to the similar method reported in the literature [21]. 7.025 g of aluminum precursor (aluminum sec-butoxide from Sigma-Aldrich) was dissolved in 60 ml of ethanol at 80 °C under vigorous stirring in a 250 ml glass bottle. For partial hydrolysis of aluminum precursor solution, 0.1 ml of nitric acid and 0.3 ml of distilled water, which had been diluted with 40 ml ethanol, were added into the solution. After maintaining the resulting solution at 80 °C for a few minutes, a clear sol was obtained. The clear sol was cooled to 50 °C. Known amounts of nickel precursor (nickel acetate tetrahydrate from Sigma-Aldrich) and second metal (M) precursor (metal acetate hydrate from Sigma-Aldrich) were then simultaneously added into the sol to obtain a nickel–M–alumina composite sol. Nickel loading and second metal loading in the nickel–M–alumina composite sol were fixed at 35 and 5 wt%, respectively. After cooling the nickel–M–alumina composite sol to room temperature, a monolithic gel was obtained by adding 25 ml of water diluted with ethanol (5 ml) into the sol. The gel was aged for 7 days, and then it was dried for a few days at 70 °C. After grinding the dried gel, it was finally calcined at 700 °C for 5 h in an air stream to yield the mesoporous nickel–M–alumina xerogel catalyst. The prepared mesoporuos nickel–M–alumina xerogel catalysts were denoted as 35Ni5MAX (M = Fe, Zr, Ni, Y, and Mg).

2.2 Characterization

Chemical compositions of 35Ni5MAX catalysts were determined by ICP-AES (Shimadz, ICP-1000IV) analyses. Physical properties (surface area, pore volume, and average pore size) of the catalysts were examined using an ASAP-2010 (Micromeritics) instrument. Crystalline phases of the catalysts were investigated by XRD (Rigaku, D-MAX2500-PC) measurements using Cu–Kα radiation (λ = 1.54056 Å) operated at 50 kV and 100 mA. In order to examine the metal-support interaction in the 35Ni5MAX catalysts, temperature-programmed reduction (TPR) measurements were carried out in a conventional flow system with a moisture trap connected to a thermal conductivity detector (TCD) at temperatures ranging from room temperature to 1,000 °C with a ramping rate of 5 °C/min. For the TPR measurement, a mixed stream of hydrogen (2 ml/min) and nitrogen (20 ml/min) was used for 50 mg of catalyst sample. CO_2-TPD (temperature-programmed desorption) experiments were conducted to determine the adsorption ability of reduced 35Ni5MAX catalysts for carbon dioxide (BEL Japan, DELCAT-B). For the TPD measurement, 100 mg of each catalyst was reduced with a mixed stream of hydrogen and helium (5.07 % H_2/He, 50 ml/min) at 700 °C for 5 h, and subsequently, it was purged with pure helium (50 ml/min) at 700 °C for 30 min. The sample was then cooled to 40 °C under a flow of helium (50 ml/min). A mixed stream of carbon dioxide and helium (5.09 % CO_2/He, 50 ml/min) was injected into the reactor at 40 °C for 60 min to saturate the catalyst. Physisorbed carbon dioxide was removed at 40 °C for 30 min under a flow of helium (50 ml/min). After purging the sample, furnace temperature was increased from 35 to 550 °C at a heating rate of 10 °C/min under a flow of helium (30 ml/min). The desorbed carbon dioxide was detected using a TCD. Adsorption ability of reduced catalysts for hydrogen was measured by H_2-TPD (temperature-programmed desorption) experiments. Prior to the H_2-TPD measurements, 200 mg of each catalyst was reduced with a mixed stream of hydrogen (3 ml/min) and argon (30 ml/min) at 700 °C for 5 h. For hydrogen adsorption, the catalyst was cooled to room temperature under a mixed stream of hydrogen (3 ml/min) and argon (30 ml/min). After cooling the catalyst to room temperature, it was purged with a stream of argon (30 ml/min) for 30 min. Furnace temperature was increased from room temperature to 700 °C at a rate of 10 °C/min under a steam of argon (20 ml/min). The desorbed hydrogen was

detected using a TCD. TPSR (temperature-programmed surface reaction) experiments were carried out to determine the temperature of methane production over reduced 35Ni5MAX catalysts. Prior to the TPSR experiment, 100 mg of each catalyst was reduced at 700 °C for 5 h with a mixed stream of hydrogen (3 ml/min) and helium (30 ml/min), and subsequently, it was cooled to room temperature. After purging the catalyst for 1 h under a steam of helium (40 ml/min), carbon dioxide (20 ml) was pulsed into the reactor every minute under a flow of helium (5 ml/min) until the catalyst was saturated with carbon dioxide. The catalyst was further treated with a stream of helium (10 ml/min) to remove physisorbed carbon dioxide at room temperature for 30 min. Furnace temperature was then increased from room temperature to 500 °C at a heating rate of 10 °C/min under a mixed stream of hydrogen (1 ml/min) and helium (9 ml/min). The produced methane was detected using a GC-MSD (Agilent, MSD-6890N).

2.3 Methane Production from Carbon Dioxide and Hydrogen

Methane production from carbon dioxide and hydrogen over 35Ni5MAX catalysts was carried out in a continuous flow fixed-bed reactor. Prior to the catalytic reaction, each catalyst (50 mg) was reduced with a mixed stream of hydrogen (3 ml/min) and nitrogen (30 ml/min) at 700 °C for 5 h. Carbon dioxide and hydrogen were continuously fed into the reactor together with nitrogen carrier. Feed composition was fixed at CO_2:H_2:N_2 = 1.0:4.0:1.7 (volume ratio). Total feed rate with respect to catalyst weight was maintained at 9,600 ml/h g. Reactor was then pressurized to 10 bar with the feed. Catalytic reaction was carried out at 220 °C and 10 bar. Reaction products were analyzed with gas chromatographs (Younglin 600D and Younglin ACME 6000). Conversion of CO_2, conversion of H_2, and product selectivity were calculated according to Eqs. (1–4). Yield for CH_4 was calculated by multiplying conversion of CO_2 and selectivity for CH_4.

$$\text{Conversion of } CO_2(\%) = \frac{\text{moles of } CO_2 \text{ reacted}}{\text{moles of } CO_2 \text{ supplied}} \times 100 \quad (1)$$

$$\text{Conversion of } H_2(\%) = \frac{\text{moles of } H_2 \text{ reacted}}{\text{moles of } H_2 \text{ supplied}} \times 100 \quad (2)$$

$$\text{Selectivity for hydrocarbon } (C_n)(\%) = \frac{\text{moles of } C_n \text{ formed}}{\text{moles of } CO_2 \text{ reacted}} \times 100 \quad (3)$$

$$\text{Selectivity for CO } (\%) = \frac{\text{moles of CO formed}}{\text{moles of } CO_2 \text{ reacted}} \times 100 \quad (4)$$

3 Results and Discussion

3.1 Physicochemical Properties of 35Ni5MAX Catalysts

Physicochemical properties of 35Ni5MAX (M = Fe, Zr, Ni, Y, and Mg) catalysts are summarized in Table 1. Nickel and second metal (M) contents in the 35Ni5MAX catalysts determined by ICP-AES analyses were in good agreement with the designed values. All the 35Ni5MAX catalysts exhibited high surface area, large pore volume, and large average pore diameter, in good agreement with the previous work [21]. The above results indicate that mesoporous nickel–M–alumina xerogel catalysts were successfully prepared by a single-step sol–gel method as attempted in this work. It was found that physicochemical properties of 35Ni5MAX catalysts were slightly different depending on the identity of second metal. The slight difference in physicochemical properties of 35Ni5MAX

Table 1 Physicochemical properties of 35Ni5MAX (M = Fe, Zr, Ni, Y, and Mg) catalysts calcined at 700 °C for 5 h

Catalyst	Ni (wt%)[a]	M (wt%)[a]	Surface area (m^2/g)[b]	Pore volume (cm^3/g)[c]	Average pore size (nm)[d]
35Ni5FeAX	34.8	4.8	234.7	0.37	4.4
35Ni5ZrAX	34.5	6.3	249.0	0.37	4.0
35Ni5NiAX	40.4	0	245.9	0.35	4.2
35Ni5YAX	36.3	4.3	229.2	0.37	4.5
35Ni5MgAX	35.6	5.1	252.2	0.35	3.8

[a] Determined by ICP-AES measurement

[b] Calculated by the BET equation

[c] BJH desorption pore volume

[d] BJH desorption average pore diameter

catalysts may be due to different atomic diameter and electron structure of second metal.

3.2 Characterization of 35Ni5MAX Catalysts

Figure 1 shows the XRD patterns of 35Ni5MAX (M = Fe, Zr, Ni, Y, and Mg) catalysts calcined at 700 °C for 5 h. The calcined catalysts showed the characteristic diffraction peaks of nickel aluminate ($NiAl_2O_4$) [22]. The peaks of second metal aluminate were not distinguishable from the peaks of $NiAl_2O_4$ [23, 24]. 35Ni5ZrAX catalyst showed the additional tetragonal ZrO_2 phase [25]. However, no distinctive diffraction peaks for second metal (M = Fe, Y, and Mg) oxide were detected.

Figure 2 shows the XRD patterns of 35Ni5MAX (M = Fe, Zr, Ni, Y, and Mg) catalysts reduced at 700 °C for 5 h. All the reduced catalysts exhibited the characteristic diffraction peaks corresponding to metallic nickel. This indicates that nickel aluminate phase in the catalysts was completely reduced into metallic nickel during the reduction process. It is interesting to note that no characteristic diffraction peaks related to Mg and Y were found in the reduced 30Ni10MgAX and 30Ni10YAX catalysts. This was attributed to amorphous state or small particles of magnesium and yttrium species [26, 27]. The reduced 35Ni5FeAX catalyst showed the mixed phase of metallic nickel and Ni–Fe alloy [28]. No characteristic diffraction peaks related to metallic iron was detected in the reduced 35Ni5FeAX catalyst. It has been reported that nickel–iron

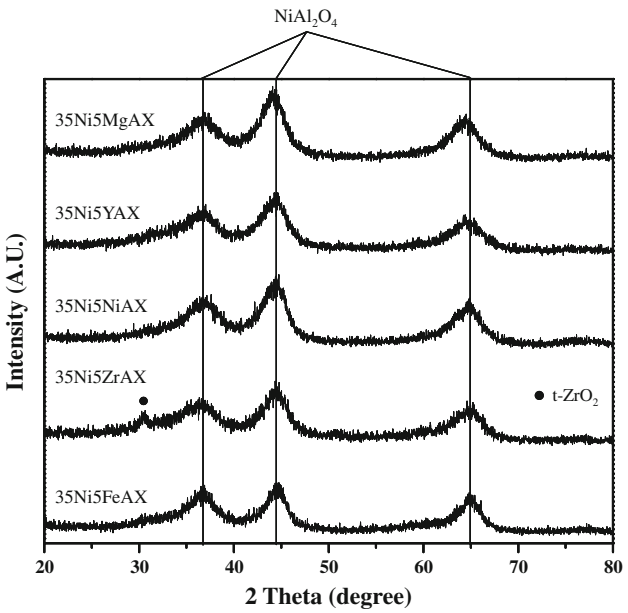

Fig. 1 XRD patterns of 35Ni5MAX (M = Fe, Zr, Ni, Y, and Mg) catalysts calcined at 700 °C for 5 h

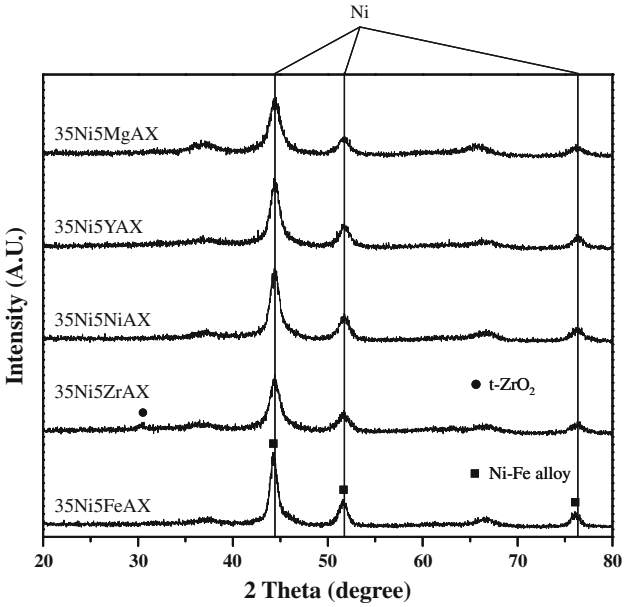

Fig. 2 XRD patterns of 35Ni5MAX (M = Fe, Zr, Ni, Y, and Mg) catalysts reduced at 700 °C for 5 h

alloy can facilitate CO dissociation on the catalyst in the methanation reaction [29]. In the reduced 35Ni5ZrAX catalyst, the characteristic diffraction peak related to tetragonal ZrO_2 was observed. This means that tetragonal ZrO_2 was not completely reduced during the reduction process. It is known that nickel catalyst supported on tetragonal ZrO_2 shows a high activity in the carbon dioxide methanation reaction [30]. It is reported that the strong interaction between oxygen vacancy in tetragonal ZrO_2 and oxygen in carbon dioxide seems to weaken C–O bond strength and to enhance carbon dioxide methanation reaction [17]. This implies that tetragonal ZrO_2 played a positive role in forming more optimal CO dissociation energy. Therefore, it is expected that 35Ni5FeAX and 30Ni5ZrAX catalysts would show a high catalytic activity in the carbon dioxide methanation reaction.

TPR measurements were carried out to investigate the metal-support interaction of 35Ni5MAX (M = Fe, Zr, Ni, Y, and Mg) catalysts, as shown in Fig. 3. Each catalyst showed a broad reduction band at around 700 °C. However, the reduction peak temperature was different depending on the identity of second metal. The reduction peak temperature increased in the order of 35Ni5FeAX < 35Ni5ZrAX < 35Ni5NiAX < 35Ni5YAX < 35Ni5MgAX. In other words, the reducibility of 35Ni5MAX catalysts decreased in the order of 35Ni5FeAX > 35Ni5ZrAX > 35Ni5NiAX > 35Ni5YAX > 35Ni5MgAX. This indicates the interaction between metal species and support was different depending on the identity of second metal. It is well known that the nature of support play a key role in the

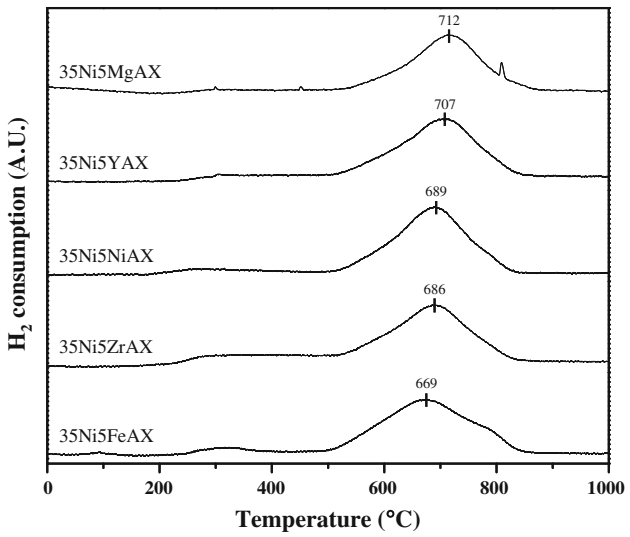

Fig. 3 TPR profiles of 35Ni5MAX (M = Fe, Zr, Ni, Y, and Mg) catalysts calcined at 700 °C for 5 h

interaction between nickel and support [31]. Thus, it can be inferred that second metal may significantly affect metal-support interaction in our catalyst system.

3.3 Catalytic Performance for Methane Production from Carbon Dioxide and Hydrogen

Catalytic performance of 35Ni5MAX (M = Fe, Zr, Ni, Y, and Mg) catalysts for methane production from carbon dioxide and hydrogen obtained at 220 °C after a 10 h-catalytic reaction is listed in Table 2. It was revealed that the catalytic performance of 35Ni5MAX catalysts was strongly influenced by the identity of second metal. Both conversion of CO_2 and yield for CH_4 decreased in the order of 35Ni5FeAX > 35Ni5ZrAX > 35Ni5NiAX > 35Ni5YAX > 35Ni5MgAX. Selectivity for CH_4 was above 99 %. High selectivity for CH_4 may be due to slow adsorption of carbon dioxide [32]. 35Ni5FeAX and 35Ni5ZrAX catalysts showed a better catalytic performance than 35Ni5NiAX catalyst in the carbon dioxide methanation reaction. This indicates that addition of iron and zirconium into mesoporous nickel–alumina xerogel catalyst was favorable for carbon dioxide methanation reaction. Among the catalysts tested, 35Ni5FeAX catalyst exhibited the best catalytic performance in terms of conversion of CO_2 and yield for CH_4.

Figure 4 shows the TEM images of 35Ni5MAX (M = Fe, Zr, Ni, Y, and Mg) catalysts after a 10 h-reaction. TEM images clearly showed that metallic species were finely dispersed in the 35Ni5MAX catalysts. Average particle size of metallic species in the reduced 35Ni5MAX catalysts was in the range of 5–10 nm with no great difference. Carbon deposition was not observed on the surface of the used 35Ni5MAX catalysts.

3.4 CO_2-TPD Experiments of 35Ni5MAX Catalysts

In order to investigate the carbon dioxide adsorption ability of the catalysts, CO_2-TPD experiments were conducted. Figure 5 shows the CO_2-TPD profiles of 35Ni5MAX (M = Fe, Zr, Ni, Y, and Mg) catalysts reduced at 700 °C for 5 h. Deconvolution analysis of TPD profiles revealed that each CO_2-TPD profile comprised three peaks. However, the amount of desorbed carbon dioxide of individual peak was not correlated with the catalytic performance. Instead, the total amount of desorbed carbon dioxide within whole temperature range (35–550 °C) was well correlated with the catalytic performance. The amount of desorbed carbon dioxide determined from total peak area of CO_2-TPD profile is summarized in Table 3. The amount of desorbed carbon dioxide was greatly influenced by the identity of second metal. The amount of desorbed carbon dioxide decreased in the order of 35Ni5MgAX > 35Ni5YAX > 35Ni5NiAX > 35Ni5ZrAX > 35Ni5FeAX. This indicates that carbon dioxide adsorption ability of the catalyst was different depending on the identity of second metal. It has been reported that electron-deficient metal particles are more active in CO_x methanation reaction than electron-rich metal particles [33]. In the case of basic support, a strong metal-support interaction, which might generate a charge transfer between metal and support, should yield an electron-rich metal surface. This implies that the difference in metal-support interaction derived

Table 2 Catalytic performance of 35Ni5MAX (M = Fe, Zr, Ni, Y, and Mg) catalysts for methane production from carbon dioxide and hydrogen obtained at 220 °C after a 10 h-catalytic reaction

Catalyst	Conversion (%)		Selectivity (%)				CH_4 yield (%)
	CO_2	H_2	C_1	C_2	C_3	CO	
35Ni5FeAX	63.4	68.3	99.5	0.5	0	0	63.1
35Ni5ZrAX	61.6	66.8	99.1	0.8	0.1	0	61.0
35Ni5NiAX	61.1	66.0	99.2	0.7	0.1	0	60.6
35Ni5YAX	58.4	61.9	99.5	0.5	0	0	58.1
35Ni5MgAX	54.2	56.6	99.5	0.4	0.1	0	53.9

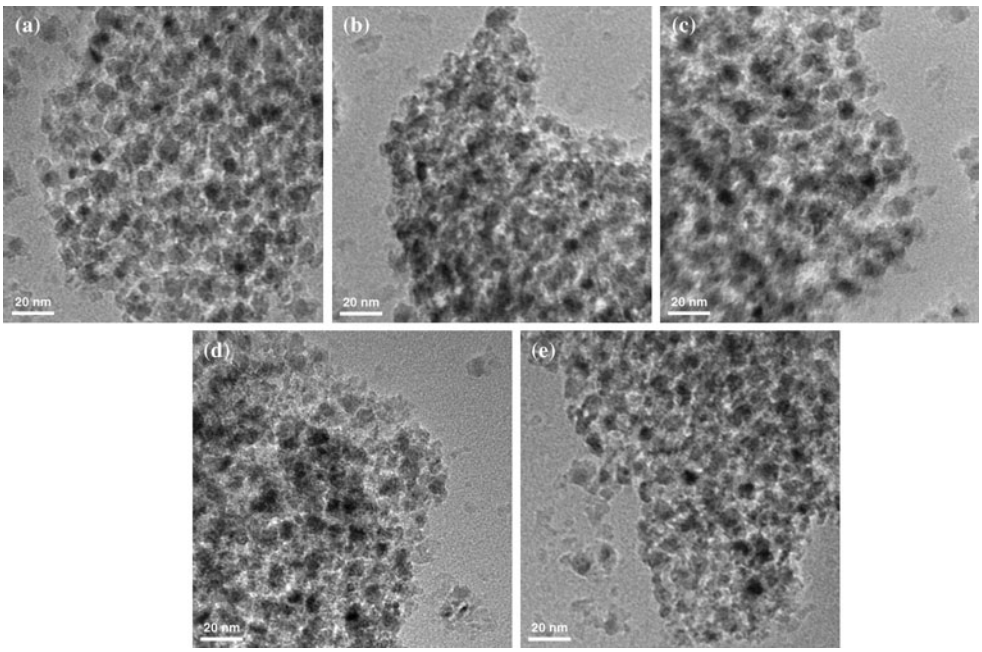

Fig. 4 TEM images of **a** 35Ni5FeAX, **b** 35Ni5ZrAX, **c** 35Ni5NiAX, **d** 35Ni5YAX, and **e** 35Ni5MgAX catalysts obtained after a 10 h-reaction

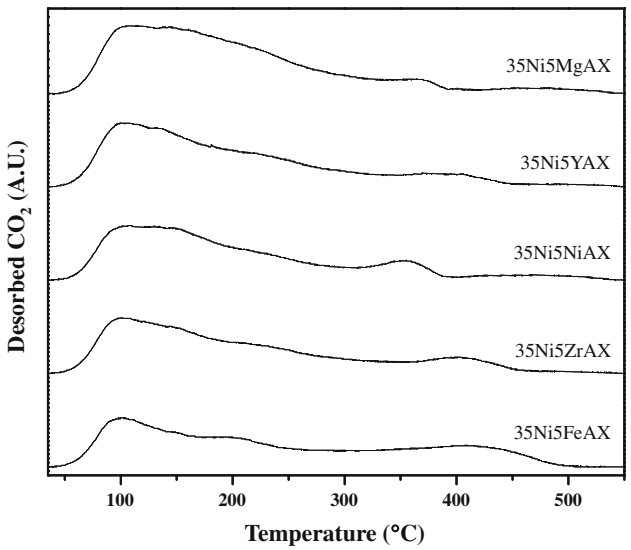

Fig. 5 CO_2-TPD profiles of 35Ni5MAX (M = Fe, Zr, Ni, Y, and Mg) catalysts reduced at 700 °C for 5 h

from different basicity of the catalyst may strongly affect the catalytic performance in the carbon dioxide methanation reaction. Because the amount of desorbed carbon dioxide corresponds to the basicity of the catalyst, it is reasonable to expect that the metal-support interaction decreased in the order of 35Ni5MgAX > 35Ni5YAX > 35Ni5NiAX > 35Ni5ZrAX > 35Ni5FeAX. Among the catalyst tested, 35Ni5FeAX catalyst retained the weakest metal-support interaction, leading to the highest catalytic performance in the carbon dioxide methanation reaction.

Table 3 Amount of desorbed CO_2 over 35Ni5MAX (M = Fe, Zr, Ni, Y, and Mg) catalysts reduced at 700 °C for 5 h

Catalyst	Amount of desorbed CO_2 (mmol-CO_2/g-catalyst)
35Ni5FeAX	0.115
35Ni5ZrAX	0.120
35Ni5NiAX	0.123
35Ni5YAX	0.144
35Ni5MgAX	0.159

Metal surface area and metal particle size of reduced 35Ni5MAX catalysts were measured by H_2-TPD experiment and the Debye–Scherrer equation, respectively. The amount of desorbed hydrogen and metal surface area of reduced catalysts are summarized in Table 4. Metal surface area decreased in the order of 35Ni5FeAX > 35Ni5NiAX > 35Ni5MgAX > 35Ni5ZrAX > 35Ni5YAX. This indicates that the amount of desorbed carbon dioxide in the CO_2-TPD experiment was not associated with the metal surface area of reduced catalysts.

Metal particle size of reduced 35Ni5MAX catalysts is also summarized in Table 4. Metal paticle size of reduced catalysts was in the range of 7.39–8.56 nm. Metal particle size increased in the order of 35Ni5FeAX < 35Ni5NiAX < 35Ni5MgAX < 35Ni5ZrAX < 35Ni5YAX. Metal particle size of reduced catalysts could not explain the difference in the amount of desorbed carbon dioxide of CO_2-TPD

Table 4 Amount of desorbed H_2 over 35Ni5MAX (M = Fe, Zr, Ni, Y, and Mg) catalysts, metal surface area, and metal particle size of 35Ni5MAX (M = Fe, Zr, Ni, Y, and Mg) catalysts reduced at 700 °C for 5 h

Catalyst	Amount of desorbed H_2 (μmol-H_2/g-catalyst)[a]	Metal surface area (m^2/g-catalyst)[b]	Metal particle size (nm)[c]
35Ni5FeAX	32.15	2.54	7.39
35Ni5ZrAX	23.49	1.84	8.04
35Ni5NiAX	26.86	2.10	7.51
35Ni5YAX	22.60	1.77	8.56
35Ni5MgAX	26.20	2.05	7.64

[a] Determined from peak area of H_2-TPD profile

[b] Calculated by the amount of desorbed H_2

[c] Calculated by the Debye–Scherrer equation

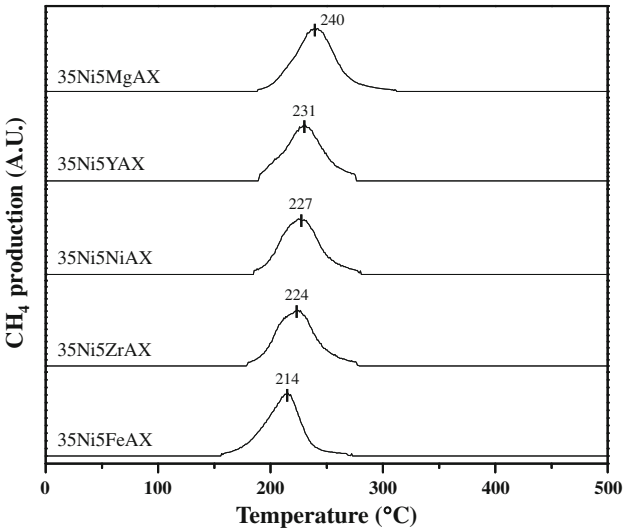

Fig. 6 TPSR profiles of 35Ni5MAX (M = Fe, Zr, Ni, Y, and Mg) catalysts reduced at 700 °C for 5 h

experiment. This indicates that the difference in the amount of desorbed carbon dioxide was influenced by the basicity of the catalyst. Thus, metal-support interaction played a key role in determining the catalytic performance.

In order to measure the basicity of calcined catalysts, we carried out additional CO_2-TPD experiments (not shown here). The amount of desorbed carbon dioxide decreased in the order of 35Ni5MgAX > 35Ni5YAX > 35Ni5NiAX > 35Ni5ZrAX > 35Ni5FeAX. This trend was well consistent with the TPR result (Fig. 3). Because reducibility was related to the chemical interaction between metal species and support in the calcined catalyst, reducibility of the catalyst was affected by the basicity of the catalyst.

3.5 TPSR Experiments of 35Ni5MAX Catalysts

In order to determine the peak temperature of methane production over the reduced 35Ni5MAX (M = Fe, Zr, Ni, Y, and Mg) catalysts in the carbon dioxide methanation reaction, TPSR experiments were carried out with an aim of elucidating the different catalytic performance. Figure 6 shows the TPSR profiles of 35Ni5MAX catalysts reduced at 700 °C for 5 h. All the catalysts showed a broad methane production peak. Methane formation appears to be limited by the dissociation of carbon monoxide to carbon species which further react with hydrogen to produce methane in the carbon monoxide methanation reaction [34]. It is known that carbon dioxide methanation reaction initially occurs by the reduction of CO_2 to CO on the catalyst surface and the dissociation of carbon monoxide to carbon species is the rate determining step [32, 35]. The reaction rate of some catalysts with high barrier for CO dissociation is limited, while the reaction rate of others with high binding energy of the adsorbed C and O species is also limited. Consequently, the catalyst used in the carbon dioxide methanation reaction needs to have an optimal CO dissociation energy to show high yield for methane [34]. It is well known that metal components in the catalyst play a key role in the dissociation of carbon monoxide to carbon species in the methanation reaction [29]. CO dissociation energy of 35Ni5MAX catalysts could be indirectly determined from peak temperature of TPSR profiles. It is inferred that a catalyst with optimal CO dissociation energy will facilitate the production of carbon species at low temperature, and subsequently, will produce methane at low temperature. Therefore, TPSR peak temperature can be used as an index for CO dissociation energy in the carbon dioxide methanation reaction. A catalyst with low TPSR peak temperature of methane production retained an optimal CO dissociation energy for producing carbon species. The lower TPSR peak temperature corresponds to the more optimal CO dissociation energy. As shown in Fig. 6, peak temperature of methane production decreased in the order of 35Ni5MgAX > 3Ni5YAX > 35Ni5NiAX > 35Ni5ZrAX > 35Ni5FeAX, in good agreement with the trend of CH_4 yield (Table 2). Among the catalyst tested, 35Ni5FeAX catalyst retained the most optimal CO dissociation energy, leading to the highest catalytic performance in the carbon dioxide methanation reaction.

3.6 Correlations Between Catalytic Performance and Catalytic Properties

Figure 7 shows the correlations between yield for CH_4 and TPSR peak temperature, and between yield for CH_4 and the amount of desorbed carbon dioxide. Yield for CH_4 was well correlated with TPSR peak temperature and with the amount of desorbed carbon dioxide. Yield for CH_4 increased with decreasing TPSR peak temperature and with

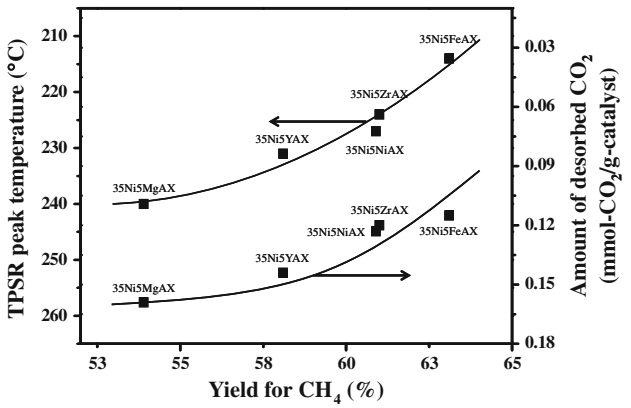

Fig. 7 Correlations between yield for CH_4 and TPSR peak temperature, and between yield for CH_4 and the amount of desorbed carbon dioxide

decreasing the amount of desorbed carbon dioxide. As mentioned earlier, the lower TPSR peak temperature and the smaller amount of desorbed carbon dioxide correspond to the more optimal CO dissociation energy of the catalyst and the weaker metal-support interaction of the catalyst, respectively. Figure 7 clearly shows that both optimal CO dissociation energy and weak metal-support interaction of the catalyst were favorable for the production of methane from carbon dioxide and hydrogen. Among the catalysts tested, 35Ni5FeAX catalyst, which retained the most optimal CO dissociation energy and the weakest metal-support interaction, exhibited the best catalytic performance in the carbon dioxide methanation reaction.

4 Conclusions

A serious of mesoporous nickel–M–alumina xerogel (35Ni5MAX) catalysts with different second metal (M = Fe, Zr, Ni, Y, and Mg) were prepared by a single-step sol–gel method, and they were applied to the methane production from carbon dioxide and hydrogen. The effect of second metal on the physicochemical properties and catalytic performance of 35Ni5MAX catalysts was investigated. Both conversion of CO_2 and yield for CH_4 decreased in the order of 35Ni5FeAX > 35Ni5ZrAX > 35Ni5NiAX > 35Ni5YAX > 35Ni5MgAX. This indicates that Fe was the most suitable second metal component (M) for 35Ni5MAX catalyst in the carbon dioxide methanation reaction. Catalytic performance of 35Ni5MAX was closely related to the CO dissociation energy (TPSR peak temperature) of the catalyst and to the metal-support interaction (the amount of desorbed carbon dioxide) of the catalyst. Yield for CH_4 increased with decreasing TPSR peak temperature and with decreasing metal-support interaction of the catalyst. Among the catalysts tested, 35Ni5FeAX catalyst, which retained the most optimal CO dissociation energy and the weakest metal-support interaction, showed the best catalytic performance in the carbon dioxide methanation reaction.

Acknowledgments This work was supported by Energy Resource R&D program (2011T100200036) under the Ministry of Knowledge Economy, Republic of Korea.

References

1. Gallagher EFJ, Euker CAJ (1980) Int J Energ Res 4:137
2. Kopyscinski J, Schildhauer TJ, Biollaz SMA (2009) Fuel 89:1763
3. Wenzhi Z, Hongjun W, Kai Q (2009) Petrol Explor Develop 36:280
4. Panagiotopoulou P, Kondarides DI, Verykios XE (2008) Appl Catal A Gen 344:45
5. Pan Z, Dong M, Meng X, Zhang X, Mu X, Zong B (2007) Chem Eng Sci 62:2712
6. Kowalczyk Z, Stołecki K, Raróg-Pilecka W, Miśkiewicz E, Wilczkowska E, Karpiński Z (2008) Appl Catal A Gen 342:35
7. Steeneveldt R, Berger B, Torp TA (2006) Chem Eng Res Des 84:739
8. Noh J, Chang J-S, Park J-N, Lee KY, Park S-E (2000) Appl Organometal Chem 14:815
9. Aaron D, Tsouris C (2005) Sep Sci Technol 40:321
10. Wang W, Wang S, Ma X, Gong J (2008) Chem Soc Rev 40:3703
11. Krylov OV, Mamedov AK (1995) Russ Chem Rev 64:877
12. Ocampo F, Louis B, Kiwi-Minsker L, Roger A-C (2011) Appl Catal A Gen 392:36
13. Wang JB, Chen P-M, Huang T-J (2001) J Chin Inst Chem Eng 32:303
14. Inui T, Funabiki M, Suehiro M, Sezume T (1979) J Chem Soc Faraday Trans 1(75):787
15. Perkas N, Amirian G, Zhong Z, Teo J, Gofer Y, Gedanken A (2009) Catal Lett 130:455
16. Kodama T, Kitayama Y, Tsuji M, Tamaura Y (1997) Energy 22:183
17. Takanoa H, Izumiyaa K, Kumagaia N, Hashimotob K (2011) Appl Surf Sci 257:8171
18. Ando H, Fujiwara M, Matsumura Y, Miyamura H, Souma Y (1995) Energy Convers Mgmt 36:653
19. Abouarnadasse S, Pajonk GM, Germain JE, Teichner SJ (1984) Appl Catal 9:119
20. Seo JG, Youn MH, Bang Y, Song IK (2010) Int J Hydrogen Energ 35:12174
21. Hwang S, Lee J, Hong UG, Seo JG, Jung JC, Koh DJ, Lim H, Byun C, Song IK (2011) J Ind Eng Chem 17:154
22. Seo JG, Youn MH, Lee H-I, Kim JJ, Yang E, Chung JS, Kim P, Song IK (2008) Chem Eng J 141:298
23. Huang L, Xie J, Chen R, Chu D, Chu W, Hsu AT (2008) Int J Hydrogen Energy 33:7448
24. Montouillout V, Massiot D, Douy A, Coutures JP (1999) J Am Ceram Soc 82:3299
25. Yamasaki M, Habazaki H, Yoshida T, Akiyama E, Kawashima A, Asami K, Hashimoto K, Komori M, Shimamura K (1997) Appl Catal A Gen 163:187
26. Sharma PK, Jilavi MH, Nab R, Schmidt H (1998) J Mater Sci Lett 17:823
27. Utamapanya S, Klabunde KJ, Schlup JR (1991) Chem Mater 3:175
28. Chicinaş I, Pop V, Isnard O, Breton JML, Juraszek J (2003) J Alloy Compd 352:34

29. Kustov AL, Frey AM, Larsen KE, Johannessen T, Nørskov JK, Christensen CH (2007) Appl Catal A Gen 320:98
30. Yamasaki M, Habazaki H, Asami K, Izumiya K, Hashimoto K (2006) Catal Commun 7:24
31. Chang FW, Kuo MS, Tsay MT, Hsieh MC (2003) Appl Catal A Gen 247:309
32. Falconer JL, Zağli AE (1980) J Catal 62:280
33. Kowalczyk Z, Stołecki K, Raróg-Pilecka W, Miśkiewicz E, Wilczkowska E, Karpiński Z (2008) Appl Catal A Gen 342:35
34. Bligaard T, Nørskov JK, Dahl S, Matthiesen J, Christensen CH, Sehested J (2004) J Catal 224:206
35. Zağli E, Falconer JL (1981) J Catal 69:1